Desalination and Water Treatment
www.deswater.com

doi: 10.5004/dwt.2021.27853

242 (2021) 304–315
December

Investigation of adsorption behavior of cationic nonwoven textiles as an alternative and environmentally friendly adsorbent to remove the Reactive blue 21 dye from a model solution

Tuğçe Demirel[a,*], Yusuf Yavuz[a], Mustafa Erdem Üreyen[b], Ali Savaş Koparal[c]

[a]*Eskişehir Technical University, Department of Environmental Engineering, Eskişehir, Turkey, Tel. 0090 222 321 35 50; emails: tdemirel@eskisehir.edu.tr (T. Demirel), yuyavuz@eskisehir.edu.tr (Y. Yavuz)*
[b]*Eskişehir Technical University, Department of Fashion Design, Eskişehir, Turkey, email: meureyen@eskisehir.edu.tr (M.E. Üreyen)*
[c]*Health Programs Department, Open Education Faculty, Anadolu University, Yunus Emre Campus, 26470, Eskisehir, Turkey, email: askopara@anadolu.edu.tr (A.S. Koparal)*

Received 16 June 2021; Accepted 26 September 2021

ABSTRACT

This study investigates the usability of cheap, easy-to-use and environmentally-friendly cationic nonwoven textiles as an alternative to the current adsorbents for the removal of dyestuffs from the colored wastewater generated by both industrial and domestic use. The parameters impacting the adsorption were analyzed to determine the efficacy of nonwoven textiles, and it was found that 99.47% of the dye could be removed under optimal conditions. The fit with Langmuir isotherm models of the Reactive blue 21 dye's adsorption onto a cationic nonwoven textile was analyzed, along with its adsorption kinetics and thermodynamics fitting the second-order rate model. The desorption studies performed for the dye adsorbed nonwoven textile at 50°C and 100°C were shown that the product was suitable for industrial use. This study puts forward an economic solution to environmental issues related to color removal through a product whose efficiency has been determined, and which we believe with contributing to a sustainable environment.

Keywords: Adsorption; Cationic nonwoven textile; Color fastness; Dyestuff; Wastewater treatment

1. Introduction

Dye-containing waters that result from, and are discharged by, various industrial processes such as textile, paper and printing industries give rise to significant problems related to environmental and human health [1,2]. Given the quantity and composition of the wastewater they produce, the textile, dyeing and finishing processes are the most polluting compared to the other sectors [3,4]. As a result of the increasing quantity and variety of production activities involving dyeing processes due to growing consumer demand, complex structures of various types and numbers are appearing in industrial wastewater [5]. More than 7×10^5 tons of dye is manufactured each year, 10%–15% of which is released as wastewater output of dyeing processes. Dyeing processes are of significant importance to the environment due to their heavy use of water, the salts used for dye fixation, the heavy metals found in some dyes and the high amount of unfixed dyes released into the wastewater [6,7]. The discharge of wastewater into receiving waters causes environmental problems, including an increase in chemical oxygen demand and toxicity in water, reduced light penetration and damage to photosynthetic life [8].

Wastewaters that contain dyes are treated through physical, chemical and biological treatment systems [9]; however, these types of treatment processes come with

* Corresponding author.

some disadvantages, such as high maintenance and operational expenses, high amounts of energy consumption, the creation of sludge and secondary pollutants, as well as a lack of effectiveness in remediating wastewater containing different types of dyestuff [10,11]. Reactive dyes are commonly used in the textile sector, especially for the dyeing of natural and regenerated cellulosic yarns and fabrics, and a 90% fixation of reactive dyes on cellulosic materials is possible in an application [12]. In such cases, it can be assumed that approximately 10% of the colorants that need to be treated prior to discharge enter the environment from the dye house wastewater [13]. Since the efficiency of dye removal differs based on the type of dye in the wastewater, selecting the best method for the elimination of color from wastewater can be difficult [14]. Adsorption is preferred to other methods of dye removal, for reasons that include lower cost, simple design, high efficiency, easy operability and a high dye removal capacity [15].

For the removal of color, a number of cheap and environmentally-friendly adsorbents are being developed as alternatives to the high-cost approaches that make use of activated carbon, which are uneconomical despite their high adsorption capacity, wide surface coverage and microporous structure [16].

Natural materials such as nanoclay [17], kaolinite [18], montmorillonite [19], bioadsorbents such as chitosan [20] fungi [21] and biomass [22], as well as agricultural and industrial wastes such as cashew nut shells [23], olive stones [24], lemon peels [25], fly ash [26], red mud [27] and sawdust [28] are among the adsorbents that have been tested in literature for the removal of dye, as an alternative to the traditional adsorbent approaches [29]. There are ongoing studies aimed at determining the adsorption capacity of these new adsorbents, and at keeping the adsorbent dosage and the resulting wastewater to a minimum [30].

In this study; cheap, easy-to-use and environmentally-friendly cationic nonwoven textiles were analyzed as an alternative to the existing processes in the removal of dyestuffs for both industrial and domestic use.

2. Materials and methods

2.1. Chemicals and reagents

Reactive dyes were used in the present study, as they are used in the production of more than 50% of all cotton fibers, despite cotton textiles being environmentally-friendly [31]. The reactive dye used in the study was Setazol Turquoise Blue (C.I. RB21) (98%), which was procured from Setaş Kimya Sanayi A.Ş. in Turkey.

The dye solutions used in the present study were obtained through a suitable dilution of a 1 g/L stock solution. All solutions were prepared in distilled water.

Sodium chloride (99.5%), sodium hydroxide (97%) and hydrochloric acid (37%) were purchased from Merck (Darmstadt, Germany).

2.2. Nonwoven textiles

A color scavenging cationic agent was applied to the nonwoven textile (90:10 viscose/polyester) samples (trade name is IZI-WASH) obtained from EGD Tekstil A.Ş. in Turkey. A quaternary ammonium salt-based cationic agent was applied to the nonwoven textile through the exhaust method.

2.3. Point of zero charge determination

The point of zero charge (pH_{pzc}) of the cationic nonwoven was determined by the pH drift method [32]. The pH of the 0.01 M NaCl solution was adjusted to a value between 2 and 12 using 0.1 M HCl or 0.1 M NaOH. A cationic nonwoven (0.15 g) was added to 50 mL of the pH adjusted solution in a capped vial. Nitrogen was bubbled through the solution at 25°C to remove dissolved carbon dioxide (CO_2) until the initial pH stabilized. The final pH, reached after 24 h in shaking incubator (Zhicheng ZHWY-2102C, China) was measured (Thermo Scientific Orion 3-Star, USA) and the change in pH (final pH–initial pH) vs. initial pH was plotted for the determination of the pH_{pzc}.

2.4. Batch studies

The parameters affecting adsorption in nonwoven textiles and those relating to isotherms were evaluated in a batch system. The parameters affecting adsorption that were studied included the amount of adsorbent, the initial dye concentration, the contact time and the effect of temperature.

The maximum wavelength of the dye and the point at which the solution-dye concentrations reached equilibrium were determined through the use of a UV-Vis spectrophotometer (Shimadzu UV1700, Japan). The maximum wavelength of the Reactive blue 21 (RB21) dye was determined to be 661 nm.

The analysis of the parameters affecting adsorption was performed in a shaking incubator using 200 mL samples and a 125 rpm mixing speed at the natural pH (pH 5.78) of the solution. Trials were conducted at 10°C, 25°C and 50°C, based on the seasonal temperatures that can be observed under the operating conditions of the wastewater treatment plants in the textile industry.

The isotherm studies were carried out in a shaking incubator at the specified temperatures, with different amounts of adsorbent (0.1–0.9 g) added to solutions with 100 mg/L of initial dilution.

The amount of RB21 adsorbed from a nonwoven unit and the dye removal efficiency percentage were calculated using Eqs. (1) and (2) [33].

$$q_e = \frac{\left(C_0 - C_e\right)V}{m} \tag{1}$$

$$\text{Removal efficiency}\left(\%\right) = \frac{\left(C_0 - C_e\right)}{C_0} \times 100 \tag{2}$$

where q_e is the equilibrium adsorption capacity of adsorbent (mg/g), C_0 is the initial RB21 concentration (mg/L), C_e is the equilibrium RB21 concentration (mg/L), V is the volume of RB21 solution (L), and m is the adsorbent amount (g).

2.5. Desorption studies

Desorption studies were performed at 50°C and 100°C. In these studies, samples were taken over a period of 120 min after placing in 500 mL of pure water a textile material that had adsorbed 1 g of RB21 dye. The absorbance of the samples taken at regular periods was measured with a spectrophotometer, from which the amount of RB21 released from the textile was determined.

The amount of dye desorbed at 50°C and 100°C at the end of 120 min from the RB21-absorbed nonwoven textile was calculated based on Eq. (3) [34].

$$\text{Desorption}(\%) = \frac{\text{Mass of dye desorbed}}{\text{Mass of dye adsorbed}} \times 100 \quad (3)$$

3. Results and discussion

During this study, the viscose polyester fiber composition of the nonwoven textiles was determined with scanning electron microscopy (Zeiss Supra 50 VP, Germany). The viscose polyester fibers comprising the nonwoven textile are shown in Fig. 1.

It is known that the adsorption properties of textile materials and thus nonwoven fabrics are affected by the geometrical characteristics of fibers and structural characteristics of fabrics [35,36]. Fig. 1 illustrates the viscose polyester fiber composition of the nonwoven textiles and fiber distribution in investigated nonwoven fabrics with different magnifications.

In order to understand the adsorption mechanism, it is necessary to determine the point of zero charge of the adsorbent. The pH_{pzc} of cationic nonwoven was determined as shown in Fig. 2. It was found that pH at 5.8 was a point of zero charge, the pH value at which the surface became neutral.

According to Fig. 2, the point of zero charge (pH_{pzc}) which indicates the surface became neutral of cationic nonwoven fabric is at approximately pH 5.8. It also shows that the cationic nonwoven adsorbent is loaded with a positive charge if the pH value of the wastewater is in the range of 2–5.8, while when the pH value of the wastewater is in the range of 5.8–12, it is negatively charged. Park and Na [37] reported that the point of zero charge (pH_{pzc}) of PP-g-AA-Am fabric was at approximately pH 9.5 ± 0.1 and they stated that the surface of PP-g-AA-Am fabric was covered with a positive charge for stated pH conditions between pH 2.5 and pH 9.0 in their study. In another study, Wang et al. [38] indicated that the surface of untreated non-woven viscose material has a negative charge in the dye liquor, however, the decolorization rate of the cationic modified only material is bigger than that of the untreated material due to its positively charged surface site on the sorbent favors the sorption of negatively charged anionic pollutants due to electrostatic attraction. As stated in the literature, the surface of the cationic nonwoven fabric charged weekly positive in our experimental pH conditions (pH 5.78) supplying higher anionic reactive dye removal.

3.1. Effect of adsorbent concentration

The effect of adsorbent quantity on the adsorption of RB21 onto nonwoven textile was analyzed by adding adsorbent in the range of 0.1–0.9 g to the solutions with an initial concentration of 100 mg/L at pH 5.78, at 125 rpm, and at temperatures of 10°C, 25°C and 50°C.

The maximum removal data on the adsorption of RB21 solutions onto nonwoven textile were calculated for 10°C, 25°C and 50°C as 98.19%, 98.89% and 99.47%, respectively. A graph presenting the data is provided in Fig. 3. An analysis of the removal data showed the optimum adsorbent dosage to be 0.5 g, as removal data between the 0.5–0.9 g adsorbent dosages were very close. It was shown that removal is increased by the increasing adsorbent concentration due to an increase of surface area until 0.5 g and then no significant increase was obtained at larger doses. It may be due to a lack of efficient contact of the dye with the increased fabric surface resulting in failure to obtain predicted treatment efficiency. Similarly, Nojavan and Gharbani [39] reported that removal is increased by the increasing dosage of adsorbent due to increase of surface area until optimum adsorbent dosage then it stayed stable due to agglomeration particles in larger amounts. In a similar study, Rana et al. [40] reported the parallel result for

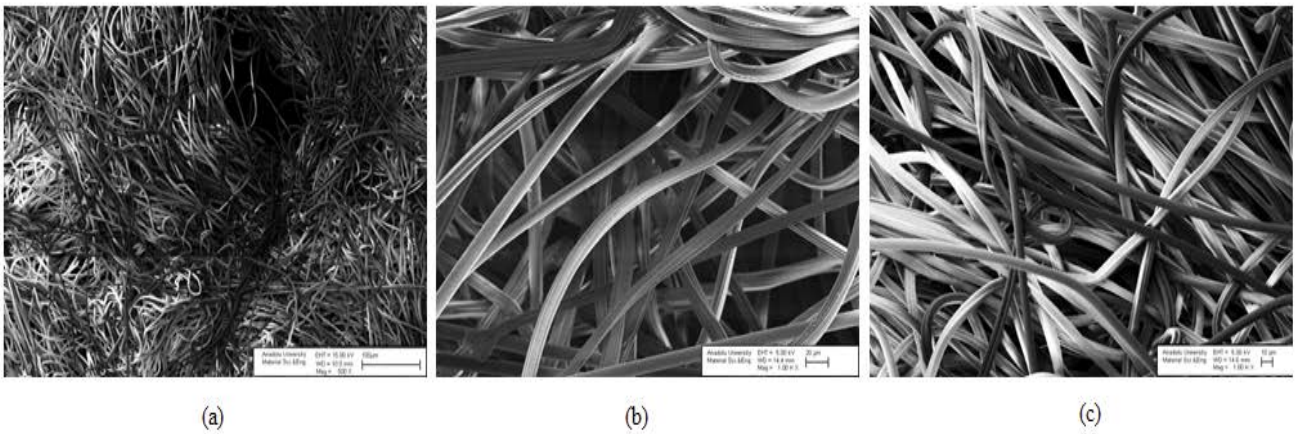

Fig. 1. Scanning electron microscopy images of (a) 500X, (b) 1.00KX, and (c) 1.00KX nonwoven textile samples.

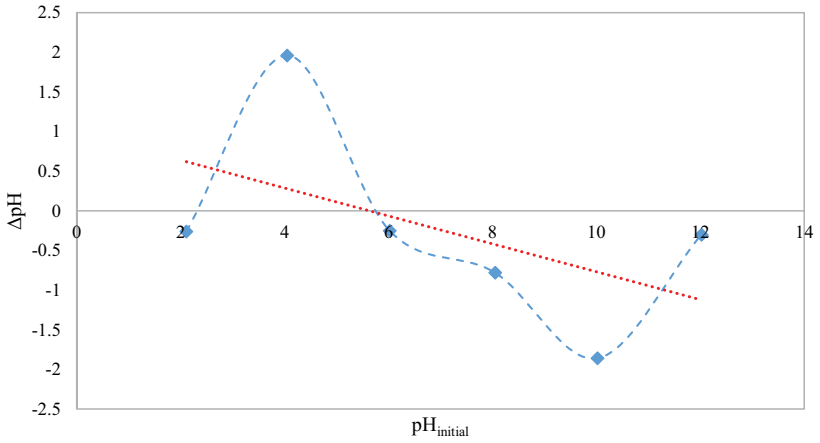

Fig. 2. Determination of pH_{pzc} of cationic nonwoven.

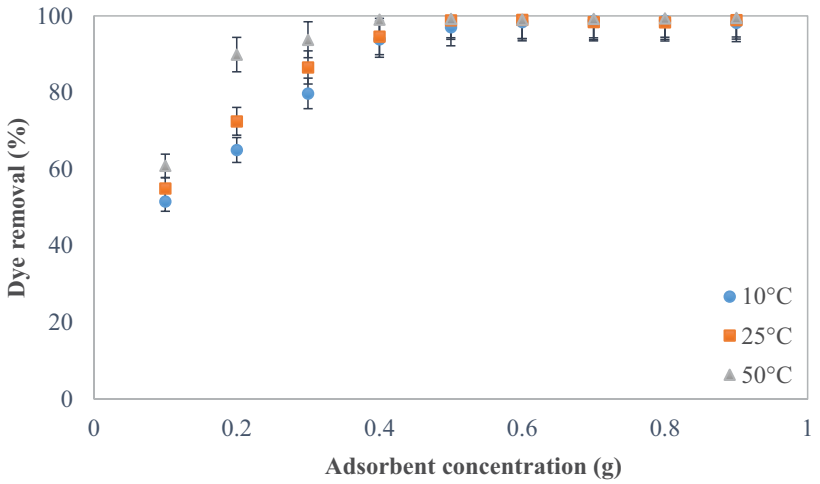

Fig. 3. Effect of adsorbent concentration for the adsorption of RB21 onto the nonwoven textile.

methylene blue dye from wastewater with sulfonated nonwoven PE Fabric due to due to the reduction of the external area of the reaction site in unit weight. When the effect of adsorbent weight was examined, it was seen that the results presented in this article were consistent with the previous literature.

3.2. Effect of temperature and contact time

The effect of temperature and contact time on the adsorption of RB21 onto nonwoven textile was analyzed at the initial concentration of 100 mg/L at pH 5.78, by adding 0.5 g of adsorbent at 10°C, 25°C and 50°C. The effect of temperature and contact time on adsorption onto nonwoven textiles is shown in Fig. 4.

The quantity of material adsorbed at the temperatures of 10°C, 25°C and 50°C by the end of 120 min was 32.87, 39.98 and 40 mg/g, respectively. This finding indicates that the quantity of material adsorbed onto the nonwoven textile showed an increase with temperature. The time of equilibrium at which the quantity adsorbed dye no longer showed a significant change with increasing temperatures was accepted as 30 min.

The temperature is an important parameter affecting the adsorption performance. Fig. 4 shows the variation of the adsorption capacity as a function of the temperature for a dye concentration of 100 mg/L and a contact time of 120 min. The variation in adsorption capacity showed the same trend for the three varied temperatures (10°C, 25°C and 50°C). The recorded decrease in adsorption performance with the gradual increase in temperature revealed that the interaction between the nonwoven adsorbent and the reactive anionic dye was exothermic [41]. This observed decrease in the adsorption capacity with the increase in temperature could be explained by the effect of the reverse stage of the mechanism and the reversibility of the interaction between the adsorbent and the dye. This may be due to the exothermic effect of the environment of the sorption process.

3.3. Effect of initial dye concentration

RB21 solutions with an initial dilution of 30–250 mg/L at pH 5.78, were contacted with 0.5 g of nonwoven textile at a 25°C temperature for 120 min, and the effect of the initial dye was dilution on adsorption was analyzed, the results of

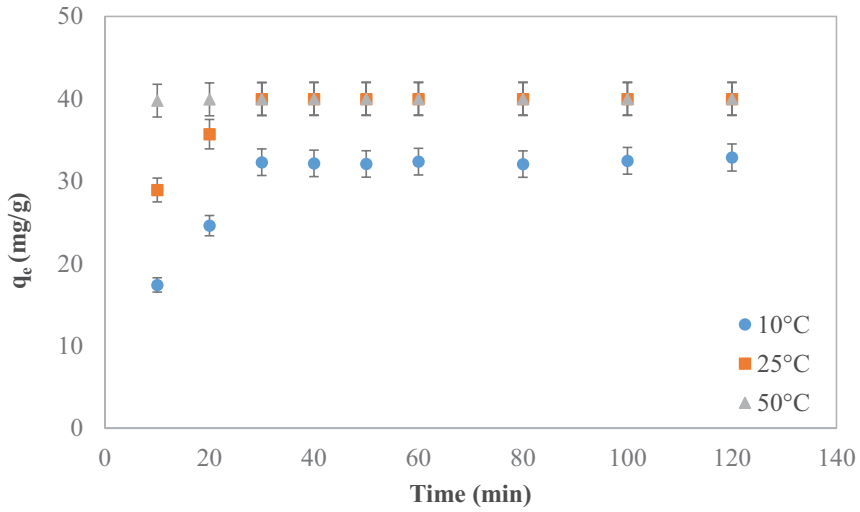

Fig. 4. Effect of temperature for the adsorption of RB21 onto the nonwoven textile.

which are shown in Fig. 5. The quantity of material adsorbed for the initial dye dilutions of 30–250 mg/L was calculated respectively as 11.98, 19.96, 40, 59.77, 79.93 and 98.49 mg/g. The quantity of material adsorbed onto the nonwoven textile showed a significant increase with increasing dye concentrations.

Fig. 5 illustrates that with the raise of RB21 concentration, the amount of RB21 absorbed per unit adsorbent also raised. When the concentration reached a higher value, all sites on the adsorbent surface became saturated. Nazia et al. [42] reported similar results for methylene blue removal acrylic acid and sodium styrene sulfonate grafted nonwoven PE Fabric. They found the linear relationship between C_e/q_e and C_e which indicates that the adsorption behavior obeys the Langmuir adsorption isotherm model using the results of the dye concentration effect on the adsorption capacity.

3.4. Adsorption isotherms

Adsorption isotherms are crucial for analyzing the adsorption process and understanding their design mechanism [43].

The fit of RB21 adsorption into the Langmuir, Freundlich and Temkin isotherm models was analyzed using adsorption equilibrium data.

The Langmuir isotherm is based on the assumptions that molecules on the surface are absorbed in one stratum, that the adsorbed molecules do not move on the surface, that the adsorption energy is the same across the surface, and that there is no interaction between the adsorbed molecules. The Langmuir isotherm is expressed by Eq. (4) [44–46].

$$q_e = \frac{q_m K_L C_e}{1 + K_L C_e} \tag{4}$$

where q_m is the maximum adsorption capacity (mg/g), K_L is the Langmuir adsorption constant (L/mg).

Eq. (5) is obtained through the linearization of the Langmuir equation.

$$\frac{C_e}{q_e} = \frac{C_e}{q_m} + \frac{1}{K_L q_m} \tag{5}$$

The plot C_e/q_e vs. C_e for the adsorption of RB21 dye on nonwoven textile in the Langmuir isotherm model is shown in Fig. 6. The Langmuir isotherm constants q_m and K_L were calculated based on this plot. The maximum adsorption capacities calculated at the temperatures of 10°C, 25°C and 50°C are given in Table 1 as 68.97, 89.29 and 129.87 mg/g, respectively, while the K_L values are given for the same temperatures as 0.322, 0.252 and 0.303 L/mg, respectively. The correlation coefficients given in Table 1 for the temperatures of 10°C, 25°C and 50°C are 0.987, 0.981 and 0.985, respectively, indicating a fit to the Langmuir isotherm model.

Dimensionless equilibrium factors such as R_L were calculated using Eq. (6).

$$R_L = \left(\frac{1}{1 + K_L C_0} \right) \tag{6}$$

The adsorption process is unfavorable when R_L is greater than 1; linear when R_L is equal to 1; favorable when R_L is between 0 and 1; and irreversible when R_L is 0 [47]. The R_L values calculated at the temperatures of 10°C, 25°C and 50°C using Eq. (6) were 0.030, 0.039 and 0.032, respectively, and these values were between 0 and 1, indicating that adsorption was favorable.

In the Freundlich isotherm model, adsorption on an adsorption surface is heterogeneous, and this isotherm model is expressed with Eq. (7).

$$q_e = K_F C_e^{1/n} \tag{7}$$

where K_F is the adsorption constant that indicates the adsorption capacity (mg/g (L/mg)$^{1/n}$), n is the adsorption constant that indicates adsorption intensity.

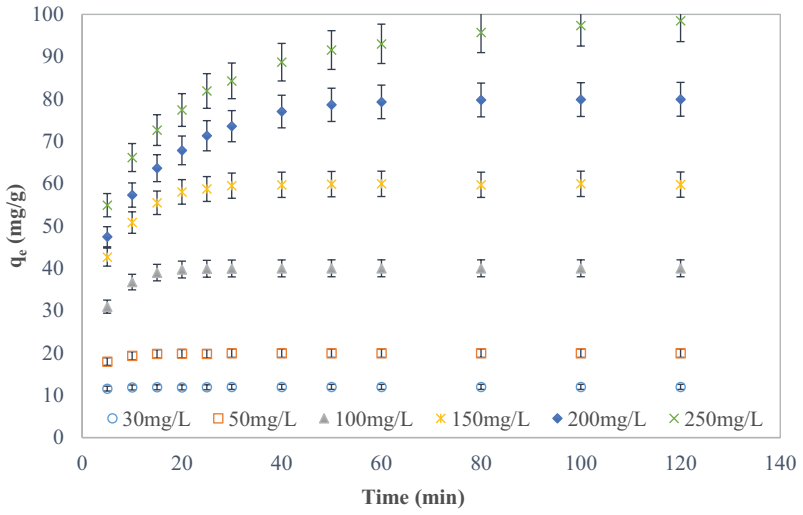

Fig. 5. Effect of initial dye concentration on the adsorption of RB21 onto the nonwoven textile.

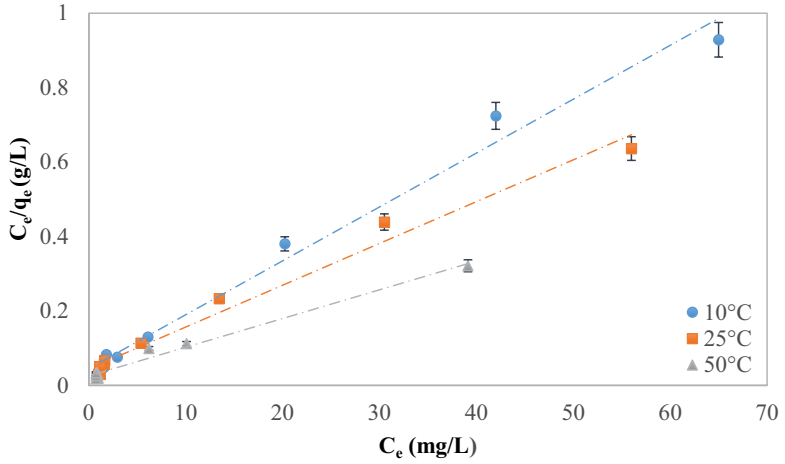

Fig. 6. Langmuir plots for the adsorption of RB21 onto nonwoven textile at various temperatures.

The linear form equation for the Freundlich isotherm is given in Eq. (8).

$$\ln q_e = \ln K_F + \frac{1}{n}\ln C_e \tag{8}$$

The plot of $\ln q_e$ vs. $\ln C_e$ is used to calculate Freundlich isotherm constants K_F and n, in which K_F indicates adsorption capacity, while n expresses favorability to the adsorption process. The slope of $1/n$ showed adsorption intensity or surface heterogeneity and lay within the range of 0 to 1. Heterogeneity increased as this value came closer to 0 [48,49].

The RB21 dye adsorption data in the Freundlich isotherm model is given in Table 1, and it was observed that it did not fit the Freundlich isotherm model due to the low values of correlation coefficients. As such, the Freundlich isotherm plot was not provided.

The Temkin isotherm, which involves interactions between adsorbed materials and which was developed by considering the adsorption enthalpy of all molecules within the solution, is as expressed by Eq. (9).

$$q_e = \frac{RT}{b}\ln\left(K_t C_e\right) \tag{9}$$

Eq. (9) can be rearranged into a linear form as:

$$q_e = B\ln K_t + B\ln C_e \tag{10}$$

here,

$$B = \frac{RT}{b} \tag{11}$$

where T is the absolute temperature (K), and R is the ideal gas constant (8.314 J/mol K) [50]. B and K_t were calculated from the slope and intercept of the linear plot $\ln q_e$ vs. $\ln C_e$. It was observed that the adsorption of RB21 did not fit the Temkin isotherm model due to the low values of the correlation coefficients given in Table 1 for 10°C, 25°C and 50°C. Thus, the Temkin isotherm plot was not provided.

Table 1
Langmuir, Freundlich and Temkin isotherm constants for the adsorption of RB21

Temp.	10°C	25°C	50°C
	Langmuir		
q_m	68.97	89.29	129.87
K_L	0.322	0.252	0.303
R^2	0.987	0.981	0.985
R_L	0.030	0.038	0.032
	Freundlich		
n	4.170	3.514	2.723
K_F	25.80	27.24	33.89
R^2	0.864	0.849	0.847
	Temkin		
K_t	11.12	6.469	5.124
B	10.14	13.76	22.04
R^2	0.929	0.910	0.929

Table 2 compares the maximum adsorption capacities of different adsorbents that were determined with the Langmuir isotherm model in previous studies from the literature on the removal of the RB21 dye.

Mohammadi et al. [57] reported that the kinetics and isotherm studies of Reactive blue 21 dye and $Ni_{0.5}Zn_{0.5}Fe_2O_4$ magnetic nanoadsorbent system and they obtained that the best fit was found to be Langmuir isotherm model for this adsorption process following the pseudo-second-order kinetics model. Also, Nojavan and Gharbani [39] adsorption reported that the response surface methodology for optimizing adsorption process parameters of Reactive blue 21 onto modified kaolin, and they indicated that RB21 onto K-CTAB was obeyed of Langmuir isotherm and adsorption kinetics of RB21 onto K-CTAB was pseudo-second-order. The results presented in this article appeared to be consistent with the literature.

3.5. Kinetics of adsorption

Given the importance of adsorption kinetics in determining adsorption efficiency, various kinetics models were used. To identify the adsorption steps that affect the adsorption of RB21, equilibrium data was analyzed using the pseudo-first-order kinetic model and the pseudo-second-order kinetic model [58].

The pseudo-first-order kinetic model specified by Lagergren is provided in Eq. (12).

$$\frac{dq_t}{dt} = k_1\left(q_e - q_t\right) \tag{12}$$

Eq. (13) was obtained by integrating and rearranging Eq. (12) while applying the boundary conditions $q_t = 0$ at $t = 0$ and $q_t = q_t$ at $t = t$.

$$\log\left(q_e - q_t\right) = \log q_e - \left(\frac{k_1}{2.303}\right)t \tag{13}$$

Table 2
Langmuir isotherm capacities for the removal of RB21 with various adsorbents

Adsorbent	Adsorption capacity (mg/g)	Reference
Fly ash	106.72	[51]
Sepiolite	66.67	[51]
Acid-treated palm shell powder	24.866	[52]
Chitosan	70.028	[52]
TiO_2	22.79	[53]
Clay	40.385	[54]
Activated clay	34.758	[54]
Modified clay	46.511	[54]
Polyurethane foam	8.31	[55]
Clinoptilolite	9.652	[56]
Cationic nonwoven	129.87	In this study

where k_1 is the pseudo-first-order rate constant (1/min).

The q_e and k_1 values were calculated from the slope and intercept of the plot log $(q_e - q_t)$ vs. t. The plot of the pseudo-first-order kinetic model was not provided due to the low values of the correlation coefficients, while the q_e, k_1 and R^2 values for this model are given in Table 3.

The pseudo-second-order kinetic model is given by Eq. (14), which is shown below.

$$\frac{dq_t}{dt} = k_2\left(q_e - q_t\right)^2 \tag{14}$$

where k_2 is the second-order adsorption constant (g/mg min). Eq. (15) was obtained by integrating and rearranging when Eq. (14) while applying the boundary conditions $q_t = 0$ at $t = 0$ and $q_t = q_t$ at $t = t$.

$$\frac{t}{q} = \frac{1}{k_2 q_e^2} + \frac{1}{q_e}t \tag{15}$$

By transferring the equilibrium data to the plot, the q_e and k_2 values were calculated from the slope of t/q vs. t-line and the intercept of the y-axis [59,60]. The plots obtained from the pseudo-second-order kinetic model are provided in Fig. 7.

The intraparticle diffusion model was used to identify the diffusion mechanism during adsorption process. The intraparticle diffusion model is given by Eq. (16):

$$q_t = k_i\sqrt{t} + C_i \tag{16}$$

where k_i (mg g^{-1} $min^{-1/2}$) is the intraparticle diffusion constant, C_i is the constant which describes the boundary layer affects [61].

The fact that correlation coefficients of the lines obtained from the second-order kinetic model for the temperatures of 10°C, 25°C and 50°C were higher than 0.99 indicates that the adsorption of RB21 onto the nonwoven textile fitted

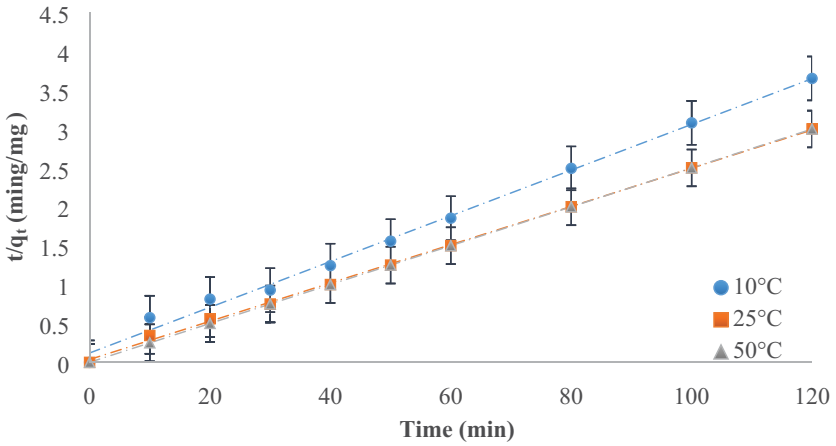

Fig. 7. Pseudo-second-order kinetic plots for the adsorption of RB21 onto the nonwoven textile.

the pseudo-second-order kinetic model as seen in Fig. 7. As presented in the intraparticle diffusion model for the temperatures of 10°C, 25°C and 50°C in Fig. 8, the intraparticle diffusion controlled the adsorption at Stage 1. Before 36 min, Stage 1 was finished and then the external surface adsorption (Stage 2) was obtained and it continued from 36 to 144 min. Generally, intraparticle diffusion rate constant k_i was the slope of the line in Stage 1. Table 3 also listed the rate parameter k_i and its correlation coefficients. There was some control of the boundary layer as it could be seen from the value of C_i. At Stage 1, this stage was a progressive process, and the rate constant k_i is the highest pointing that the intraparticle diffusion is the main controlling factor of adsorption rate for the 10°C, and it was seen that intraparticle diffusion effect on adsorption was reduced with temperature rise. In parallel with these presented findings, Nazia et al. [42] reported the methylene blue removal with acrylic acid and sodium styrene sulfonate grafted nonwoven PE Fabric adsorption inferring the pseudo-second-order adsorption kinetic model recommends that the intraparticle diffusion process acted as the rate-limiting step of the adsorption capacity.

3.6. Thermodynamic parameters

The standard Gibbs free energy (Δ*G*°), standard enthalpy (Δ*H*°) and standard entropy (Δ*S*°) of the adsorption process were obtained using the equations below with the data obtained at the temperatures of 10°C, 25°C and 50°C. The associated results are provided in Table 4.

$$K_C = \frac{C_A}{C_S} \tag{17}$$

$$\Delta G^\circ = -RT \ln K_C \tag{18}$$

$$\ln K_C = -\frac{\Delta H^\circ}{RT} + \frac{\Delta S^\circ}{R} \tag{19}$$

where K_C is the equilibrium constant, C_A is the RB21 concentration adsorbed at equilibrium time (mg/L), C_S is the RB21 concentration remaining in the solution at equilibrium time (mg/L), Δ*G*° is the change in free energy, *R* is the universal gas constant (8.314 J/mol), and *T*: absolute temperature (K).

The change in enthalpy (Δ*H*) and entropy (Δ*S*) calculated from the slope and intercept of the plot 1/*T* vs. InK_C, as shown in Fig. 9, is provided in Table 4 [62].

Table 4
Thermodynamic parameters for the adsorption of RB21 onto nonwoven textile at various temperatures

Temp. (°C)	Δ*G*° (kJ/mol)	Δ*H*° (kJ/mol)	Δ*S*° (J/mol K)
10	–22.85		
25	–26.38	26.00	173.71
50	–29.87		

Table 3
Kinetic parameters for the adsorption of RB21 onto nonwoven textile at various temperatures

Temp. (°C)	Pseudo-first-order kinetic model			Pseudo-second-order kinetic model			Intraparticle diffusion model		
	q_e	k_1	R^2	q_e	k_2	R^2	k_i	C_i	R^2
10	4.046	0.025	0.251	34.01	0.007	0.995	6.3897	3.1597	0.991
25	7.127	0.024	0.502	40.65	0.017	0.999	4.7935	13.9200	0.997
50	–0.0007	0.817	0.0003	40	1.042	1	0.0895	39.5030	0.946

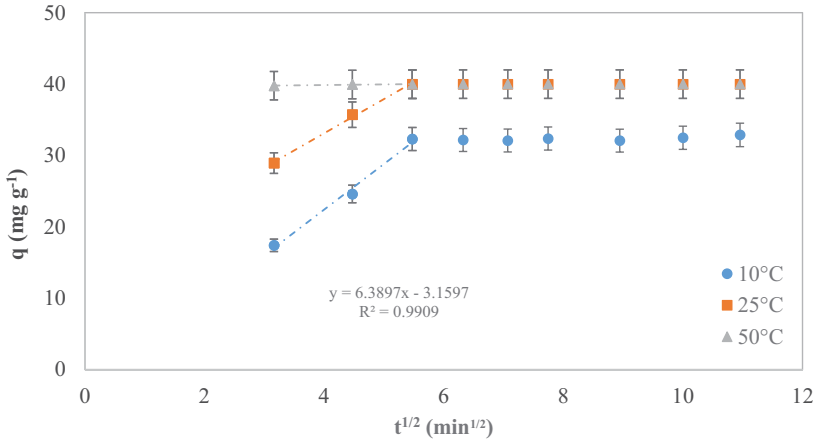

Fig. 8. Intraparticle diffusion model for the adsorption of RB21.

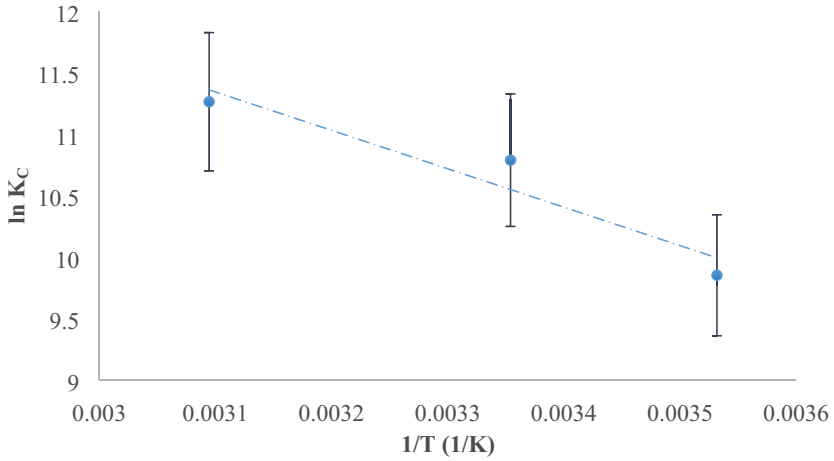

Fig. 9. Plot of lnK_C vs. 1/T for estimation of thermodynamic parameters.

A positive $\Delta H°$ (26.00 kJ/mol) indicates that the adsorption is endothermic, while a negative $\Delta G°$ for all temperatures (–22.85, –26.38 and –29.87 kJ/mol) indicates that the adsorption is spontaneous. The positive values of $\Delta S°$ mean an increase in randomness at the solid/solution interface [63,64].

3.8. Desorption

It was observed that, by the end of 120 min, 1.47% of RB21 was released at 50°C, and 37.26% of RB21 was released at 100°C from the RB21-adsorbed nonwoven textile. The plot for the RB21 desorption is given in Fig. 10. El Messaoudi et al. [65] reported similar results for the desorption efficiency of Congo red increases from 83.13% to 92.89% for dye-loaded *Phoenix dactylifera* date stones and from 77.18% to 86.27% for *Zizyphus lotus* jujube shells with increasing of the temperature from 10°C to 50°C.

4. Conclusion

The studied parameters that affected the adsorption included the amount of adsorbent, initial dye concentration, contact time and the effect of temperature. Whether the adsorption of RB21 reactive dye fitted with the Langmuir, Freundlich, and Temkin isotherm models was investigated, and it was found that the molecules on the surface were adsorbed in one stratum and fitted the Langmuir isotherm model.

The results of the study can be summarized as follows:

In a comparison of the pseudo-first-order kinetic model and pseudo-second-order kinetic model results of the dye adsorption, it was found that the correlation coefficient was significantly low in the first-order rate model, and that the adsorption kinetics fitted the second-order rate model. According to the intraparticle diffusion model for the temperatures of 10°C, 25°C and 50°C, it was determined that the adsorption mechanism was controlled by two steps: intra-particle diffusion (Stage 1) and external surface diffusion (Stage 2). A positive $\Delta H°$ indicated that the adsorption was endothermic, while a negative $\Delta G°$ for all temperatures indicated that the adsorption was spontaneous. Positive values of $\Delta S°$ indicate an increase in randomness at the solid-solution interface.

The low values of desorption for the dye adsorbed nonwoven textile at 50°C and 100°C indicate that the product is suitable for industrial use.

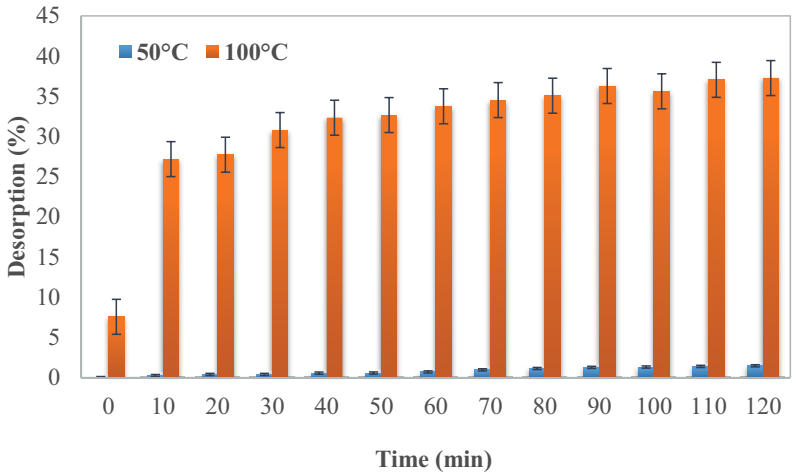

Fig. 10. Desorption of RB21 onto nonwoven textile at various temperatures.

The nonwoven textile had a greater dye adsorption capacity than many of the existing adsorbents. The use of nonwoven textiles as an adsorbent for the removal of dye from dye-containing wastewater can be considered an effective and economic method for removing dyes from textile wastewater.

Acknowledgements

This study was supported by Anadolu University Scientific Research Projects Commission. Project No: 1304F073.

References

[1] H. Daraei, A. Mittal, Investigation of adsorption performance of activated carbon prepared from waste tire for the removal of methylene blue dye from wastewater, Desal. Water Treat., 90 (2017) 294–298.
[2] J. Zhao, L. Xu, Y. Su, H. Yu, H. Liu, S. Qian, W. Zheng, Y. Zhao, Zr-MOFs loaded on polyurethane foam by polydopamine for enhanced dye adsorption, J. Environ. Sci., 101 (2021) 177–188.
[3] B. Keskin, M.E. Ersahin, H. Ozgun, I. Koyuncu, Pilot and full-scale applications of membrane processes for textile wastewater treatment: a critical review, J. Water Process Eng., 42 (2021) 102172, doi: 10.1016/j.jwpe.2021.102172.
[4] T. Shindhal, P. Rakholiya, S. Varjani, A. Pandey, H.H. Ngo, W. Guo, H.Y. Ng, M.J. Taherzadeh, A critical review on advances in the practices and perspectives for the treatment of dye industry wastewater, Bioengineered, 12 (2021) 70–87.
[5] A. Alinsafi, F. Evenou, E.M. Abdulkarim, M.N. Pons, O. Zahraa, A. Benhammou, A. Yaacoubi, A. Nejmeddine, Treatment of textile industry wastewater by supported photocatalysis, Dyes Pigm., 74 (2007) 439–445.
[6] M.A. Al-Ghouti, M.A.M. Khraisheh, S.J. Allen, M.N. Ahmad, The removal of dyes from textile wastewater: a study of the physical characteristics and adsorption mechanisms of diatomaceous earth, J. Environ. Manage., 69 (2003) 229–238.
[7] M.T. Yagub, T.K. Sen, S. Afroze, H.M. Ang, Dye and its removal from aqueous solution by adsorption: a review, Adv. Colloid Interface Sci., 209 (2014) 172–184.
[8] A.K. Moorthy, B.G. Rathi, S.P. Shukla, K. Kumar, V.S. Bharti, Acute toxicity of textile dye methylene blue on growth and metabolism of selected freshwater microalgae, Environ. Toxicol. Pharmacol., 82 (2021) 103552, doi: 10.1016/j.etap.2020.103552.
[9] S. Samsami, M. Mohamadizaniani, M.H. Sarrafzadeh, E.R. Rene, M. Firoozbahr, Recent advances in the treatment of dye-containing wastewater from textile industries: overview and perspectives, Process Saf. Environ. Prot., 143 (2020) 138–163.
[10] V. Katheresan, J. Kansedo, S.Y. Lau, Efficiency of various recent wastewater dye removal methods: a review, J. Environ. Chem. Eng., 6 (2018) 4676–4697.
[11] G. Crini, E. Lichtfouse, Advantages and disadvantages of techniques used for wastewater treatment, Environ. Chem. Lett., 17 (2019) 145–155.
[12] K. Singh, S. Arora, Removal of synthetic textile dyes from wastewaters: a critical review on present treatment technologies, Crit. Rev. Env. Sci. Technol., 41 (2011) 807–878.
[13] Y. Anjaneyulu, N.S. Chary, D.S.S. Raj, Decolourization of industrial effluents–available methods and emerging technologies–a review, Rev. Environ. Sci. Biotechnol., 4 (2005) 245–273.
[14] İ.K. Kapdan, F. Kargı, Atıksulardan tekstil boyar maddelerinin adsorpsiyonlu biyolojik arıtım ile giderimi, Turkish J. Eng. Environ. Sci., 24 (2000) 161–169.
[15] S.M. El-Kousy, H.G. El-Shorbagy, M.A. Abd El-Ghaffar, Chitosan/montmorillonite composites for fast removal of methylene blue from aqueous solutions, Mater. Chem. Phys., 254 (2020) 123236, doi: 10.1016/j.matchemphys.2020.123236.
[16] G. Crini, E. Lichtfouse, L.D. Wilson, N. Morin-Crini, Conventional and non-conventional adsorbents for wastewater treatment, Environ. Chem. Lett., 17 (2019) 195–213.
[17] S. Barakan, V. Aghazadeh, The advantages of clay mineral modification methods for enhancing adsorption efficiency in wastewater treatment: a review, Environ. Sci. Pollut. Res., 28 (2021) 2572–2599.
[18] E. Rosales, D. Anasie, M. Pazos, I. Lazar, M.A. Sanromán, Kaolinite adsorption-regeneration system for dyestuff treatment by Fenton based processes, Sci. Total Environ., 622–623 (2018) 556–562.
[19] R. Haounati, H. Ouachtak, R. El Haouti, S. Akhouairi, F. Largo, F. Akbal, A. Benlhachemi, A. Jada, A.A. Addi, Elaboration and properties of a new SDS/CTAB@ Montmorillonite organoclay composite as a superb adsorbent for the removal of malachite green from aqueous solutions, Sep. Purif. Technol., 255 (2021) 117335, doi: 10.1016/j.seppur.2020.117335.
[20] X. Zhao, X. Wang, T. Lou, Preparation of fibrous chitosan/sodium alginate composite foams for the adsorption of cationic and anionic dyes, J. Hazard. Mater., 403 (2021) 124054, doi: 10.1016/j.jhazmat.2020.124054.
[21] A. Sintakindi, B. Ankamwar, Fungal biosorption as an alternative for the treatment of dyes in waste waters: a review, Environ. Technol. Rev., 10 (2021) 26–43.
[22] A. Saravanan, S. Karishma, P.S. Kumar, S. Varjani, P.R. Yaashikaa, S. Jeevanantham, R. Ramamurthy, B. Reshma, Simultaneous removal of Cu(II) and Reactive Green 6 dye

from wastewater using immobilized mixed fungal biomass and its recovery, Chemosphere, 271 (2021) 129519, doi: 10.1016/j.chemosphere.2020.129519.
[23] P.S. Kumar, S. Ramalingam, C. Senthamarai, M. Niranjanaa, P. Vijayalakshmi, S. Sivanesan, Adsorption of dye from aqueous solution by cashew nut shell: studies on equilibrium isotherm, kinetics and thermodynamics of interactions, Desalination, 261 (2010) 52–60.
[24] M.A. Al-Ghouti, A.O. Sweleh, Optimizing textile dye removal by activated carbon prepared from olive stones, Environ. Technol. Innovation, 16 (2019) 100488, doi: 10.1016/j.eti.2019.100488.
[25] S.Z. Mohammadi, N. Mofidinasab, M.A. Karimi, F. Mosazadeh, Fast and efficient removal of Pb(II) ion and malachite green dye from wastewater by using magnetic activated carbon–cobalt nanoparticles, Water Sci. Technol., 82 (2020) 829–842.
[26] U.O. Aigbe, K.E. Ukhurebor, R.B. Onyancha, O.A. Osibote, H. Darmokoesoemo, H.S. Kusuma, Fly ash-based adsorbent for adsorption of heavy metals and dyes from aqueous solution: a review, J. Mater. Res. Technol., 14 (2021) 2751–2774.
[27] Y. Gao, J. Zhang, C. Chen, Y. Du, G. Teng, Z. Wu, Functional biochar fabricated from waste red mud and corn straw in China for acidic dye wastewater treatment, J. Cleaner Prod., 320 (2021) 128887, doi: 10.1016/j.jclepro.2021.128887.
[28] A. Khasri, M.R.M. Jamir, A.A. Ahmad, M.A. Ahmad, Adsorption of remazol brilliant violet 5R dye from aqueous solution onto melunak and rubberwood sawdust based activated carbon: interaction mechanism, isotherm, kinetic and thermodynamic properties, Desal. Water Treat., 216 (2021) 401–411.
[29] M. Rafatullah, O. Sulaiman, R. Hashim, A. Ahmad, Adsorption of methylene blue on low-cost adsorbents: a review, J. Hazard. Mater., 177 (2010) 70–80.
[30] G. Crini, P.M. Badot, Application of chitosan, a natural aminopolysaccharide, for dye removal from aqueous solutions by adsorption processes using batch studies: a review of recent literature, Prog. Polym. Sci., 33 (2008) 399–447.
[31] B.R. Babu, A.K. Parande, S. Raghu, T.P. Kumar, Cotton textile processing: waste generation and effluent treatment, J. Cotton Sci., 11 (2007) 141–153.
[32] V. Selen, Ö. Güler, D. Özer, E. Evin, Synthesized multi-walled carbon nanotubes as a potential adsorbent for the removal of methylene blue dye: kinetics, isotherms, and thermodynamics, Desal. Water Treat., 57 (2015) 8826–8838.
[33] H. Karimi-Maleh, S. Ranjbari, B. Tanhaei, A. Ayati, Y. Orooji, M. Alizadeh, F. Karimi, S. Salmanpour, J. Rouhi, M. Sillanpää, F. Sen, Novel 1-butyl-3-methylimidazolium bromide impregnated chitosan hydrogel beads nanostructure as an efficient nanobio-adsorbent for cationic dye removal: kinetic study, Environ. Res., 195 (2021) 110809, doi: 10.1016/j.envres.2021.110809.
[34] A.W.M. Ip, J.P. Barford, G. McKay, Reactive black dye adsorption/desorption onto different adsorbents: effect of salt, surface chemistry, pore size and surface area, J. Colloid Interface Sci., 337 (2009) 32–38.
[35] K.A. Asanovic, D.D. Cerovic, M.M. Kostic, S.B. Maletic, A.D. Kramar, Multipurpose nonwoven viscose/polypropylene fabrics: effect of fabric characteristics on sorption and dielectric properties, J. Polym. Sci., Part B: Polym. Phys., 56 (2018) 947–957.
[36] P.K. Patnaik, P.T.R. Swain, S.K. Mishra, A. Purohit, S. Biswas, Recent developments on characterization of needle-punched nonwoven fabric reinforced polymer composites–a review, Mater. Today:. Proc., 26 (2020) 466–470.
[37] H.J. Park, C.K. Na, Adsorption characteristics of anionic nutrients onto the PP-g-AA-Am non-woven fabric prepared by photoinduced graft and subsequent chemical modification, J. Hazard. Mater., 166 (2009) 1201–1209.
[38] X. Wang, Y. Liu, R. Lv, Preparation of a kind of non-woven viscose colour absorbing material and research of its colour absorption properties, Fibres Text. East. Eur., 3 (2019) 71–77.
[39] A. Nojavan, P. Gharbani, Response surface methodology for optimizing adsorption process parameters of Reactive blue 21 onto modified kaolin, Adv. Environ. Technol., 2 (2017) 89–98.
[40] M.S. Rana, N. Rahman, T.A. Chowdhury, N.C. Dafader, S. Sultana, M.N. Sardar, M.N. Kayser, Application of sulfonated GMA-g-nonwoven PE fabric for the efficient removal of methylene blue dye from wastewater, Am. J. Polym. Sci. Technol., 7 (2021) 1–9.
[41] Y. El-Ghoul, C. Ammar, F.M. Alminderej, M. Shafiquzzaman, Design and evaluation of a new natural multi-layered biopolymeric adsorbent system-based chitosan/cellulosic nonwoven material for the biosorption of industrial textile effluents, Polymers, 13 (2021) 322, doi: 10.3390/polym13030322.
[42] R. Nazia, D.N. Chandra, S. Shahnaz, A.F. Tasneem, M.A. Rahim, Application of acrylic acid and sodium styrene sulfonate grafted non-woven PE fabric in methylene blue removal, Res. J. Chem. Environ., 24 (2020) 36–43.
[43] Ö. Gerçel, H.F. Gerçel, A.S. Koparal, Ü.B. Öğütveren, Removal of disperse dye from aqueous solution by novel adsorbent prepared from biomass plant material, J. Hazard. Mater., 160 (2008) 668–674.
[44] S. Chen, J. Zhang, C. Zhang, Q Yue, Y. Li, C. Li, Equilibrium and kinetic studies of methyl orange and methyl violet adsorption on activated carbon derived from *Phragmites australis*, Desalination, 252 (2010) 149–156.
[45] K.Y. Foo, B.H. Hameed, Insights into the modeling of adsorption isotherm systems, Chem. Eng. J., 156 (2010) 2–10.
[46] B.H. Hameed, A.A. Ahmad, Batch adsorption of methylene blue from aqueous solution by garlic peel, an agricultural waste biomass, J. Hazard. Mater., 164 (2009) 870–875.
[47] R. Han, P. Han, Z. Cai, Z. Zhao, M. Tang, Kinetics and isotherms of neutral red adsorption on peanut husk, J. Environ. Sci., 20 (2008) 1035–1041.
[48] Y. Yao, H. Bing, X. Feifei, C. Xiaofeng, Equilibrium and kinetic studies of methyl orange adsorption on multiwalled carbon nanotubes, Chem. Eng. J., 170 (2011) 82–89.
[49] I.A.W. Tan, A.L. Ahmad, B.H. Hameed, Adsorption of basic dye on high-surface-area activated carbon prepared from coconut husk: equilibrium, kinetic and thermodynamic studies, J. Hazard. Mater., 154 (2008) 337–346.
[50] A.S. Özcan, B. Erdem, A. Özcan, Adsorption of Acid blue 193 from aqueous solutions onto BTMA-bentonite, Colloids Surf., A, 266 (2005) 73–81.
[51] E. Demirbas, M.Z. Nas, Batch kinetic and equilibrium studies of adsorption of Reactive blue 21 by fly ash and sepiolite, Desalination, 243 (2009) 8–21.
[52] G. Sreelatha, V. Ageetha, J. Parmar, P. Padmaja, Equilibrium and kinetic studies on reactive dye adsorption using palm shell powder (an agrowaste) and chitosan, J. Chem. Eng. Data, 56 (2010) 35–42.
[53] P. Srivastava, S. Goyal, R. Tayade, Ultrasound-assisted adsorption of Reactive blue 21 dye on TiO_2 in the presence of some rare earths (La, Ce, Pr & Gd), Can. J. Chem. Eng., 92 (2014) 41–51.
[54] A. Vanaamudan, N. Pathan, P. Pamidimukkala, Adsorption of Reactive blue 21 from aqueous solutions onto clay, activated clay, and modified clay, Desal. Water Treat., 52 (2013) 1589–1599.
[55] J.J.S. Neta, G.C. Moreira, C.J. da Silva, C. Reis, E.L. Reis, Use of polyurethane foams for the removal of the Direct red 80 and Reactive blue 21 dyes in aqueous medium, Desalination, 281 (2011) 55–60.
[56] T. Sismanoglu, Y. Kismir, S. Karakus, Single and binary adsorption of reactive dyes from aqueous solutions onto clinoptilolite, J. Hazard. Mater., 184 (2010) 164–169.
[57] F. Mohammadi, A.R. Kazemizadeh, M. Hekmati, A. Ramazani, P. Eskandari, Environment-friendly synthesis of $Ni_{0.5}Zn_{0.5}Fe_2O_4$ magnetic nanoparticles using *Plantago major* and its applications as an efficient and rapid adsorbent for removal of Reactive blue 21 dye, Int. J. Environ. Anal. Chem., (2021) 1–20, doi: 10.1080/03067319.2021.1877280.
[58] A.P. Vieira, S.A.A. Santana, C.W.B. Bezerra, H.A.S. Silva, J.A.P. Chaves, J.C.P. de Melo, E.C. da Silva Filho, C. Airoldi, Kinetics and thermodynamics of textile dye adsorption from aqueous solutions using babassu coconut mesocarp, J. Hazard. Mater., 166 (2009) 1272–1278.

[59] Y.C. Wong, Y.S. Szeto, W.H. Cheung, G. McKay, Pseudo-first-order kinetic studies of the sorption of acid dyes onto chitosan, J. Appl. Polym. Sci., 92 (2004) 1633–1645.
[60] S. Elemen, E.P.A. Kumbasar, S. Yapar, Modeling the adsorption of textile dye on organoclay using an artificial neural network, Dyes Pigm., 95 (2012) 102–111.
[61] A.E. Ofomaja, E.B. Naidoo, A. Pholosi, Intraparticle diffusion of Cr(VI) through biomass and magnetite coated biomass: a comparative kinetic and diffusion study, S. Afr. J. Chem. Eng., 32 (2020) 39–55.
[62] A.S. Özcan, B. Erdem, A. Özcan, Adsorption of Acid blue 193 from aqueous solutions onto Na–bentonite and DTMA–bentonite, J. Colloid Interface Sci., 280 (2004) 44–54.
[63] N.M. Mahmoodi, R. Salehi, M. Arami, H. Bahrami, Dye removal from colored textile wastewater using chitosan in binary systems, Desalination, 267 (2011) 64–72.
[64] F. Nekouei, S. Nekouei, I. Tyagi, V.K. Gupta, Kinetic, thermodynamic and isotherm studies for Acid blue 129 removal from liquids using copper oxide nanoparticle-modified activated carbon as a novel adsorbent, J. Mol. Liq., 201 (2015) 124–133.
[65] N. El Messaoudi, M. El Khomri, N. Chlif, Z.G. Chegini, A. Dbik, S. Bentahar, A. Lacherai, Desorption of Congo red from dye-loaded *Phoenix dactylifera* date stones and *Ziziphus lotus* jujube shells, Groundwater Sustainable Dev., 12 (2021) 100552, doi: 10.1016/j.gsd.2021.100552.